
Supporting Information

Aqueous-phase Fischer-Tropsch reaction for production of oxygenates from syngas over colloidal ruthenium nanoparticles

Junli Zhang[a], Fei Yu[b], Yunlei An[b], Tiejun Lin*[b], Liangshu Zhong*[a,b]

[a] School of Physical Science and Technology, ShanghaiTech University, Shanghai 201210, PR China

[b] CAS Key Laboratory of Low-Carbon Conversion Science and Engineering, Shanghai Advanced Research Institute, Chinese Academy of Sciences, Shanghai 201210, PR China

E-mail addresses: zhongls@sari.ac.cn (L. Zhong), lintj@sari.ac.cn (T. Lin).

Experimental details

Synthesis of Ru nanoparticles

In a typical experiment, $RuCl_3 \cdot nH_2O$ (0.11g, 0.4136mmol) was dissolved in 30 mL distilled water, and (PVP) polyvinyl pyrrolidone (0.31g, M_n=58000, mol ratio PVP/Ru =6) was added slowly to the solution under vigorous stirring at ambient conditions. Then 4 mL mixture of cyclohexane and decalin was added to the solution quickly and transported into a 60 mL stainless steel autoclave equipped with a high-precision pressure gauge (±0.4%). Cyclohexane was added as extractant and decalin was used as internal standard. The catalyst was reduced with 2.0 MPa H_2 at 150 °C for 2 h with a stirring speed of 1000 rpm. The resulting black solution containing Ru nanoparticles was used for the aqueous FTS. As for the Na-promoted Ru nanoparticles, a certain amount of sodium salt was added simultaneously with $RuCl_3 \cdot nH_2O$, and the other procedures are the same as that above mentioned. For the comparison of the role of anion of Na salt, 180 mg of NaCl or NaOH or $NaNO_3$ was added.

Catalytic evaluation

The AFTS reaction was conducted in a 60 mL batch autoclave reactor. After reduction, the reactor was slowly cooled down to room temperature with stirring and then flushed with syngas ($CO:H_2:N_2$=32:64:4) for 5 times, and then the reactor was pressured to 3 MPa with syngas ($CO:H_2:N_2$=32:64:4). The AFTS performance was measured at 150 °C under stirring (1000 rpm) for 5 h. The reaction was terminated by immersing the autoclave into an ice bath until the reactor was cooled down to room temperature, and the products were collected and analyzed. The autoclave was linked with gas chromatography (Agilent 7890B) equipped with thermal conductivity (TCD) detector and flame ionization (FID) detectors to give a detailed analysis of the gas products. The liquid products after separating oil and water were analyzed by Shimadzu GC2010 instrument and Agilent 7890 GC-5975 MS. The water phases were analyzed by FID for detection of C_1~C_5 oxygenates. The oil products were analyzed by FID equipped with an HP-1 column.

Structure characterization

Transmission electron microscopy(TEM) was performed on a JEOL JEM-2100F microscope operating at 200kV. Before measurement, the sample was ultrasonically dispersed for ten minutes and deposited on a holey carbon film on a Cu grid. The size distribution was determined by counting at least 100 particles for each sample.

X-ray photoelectron spectroscopy (XPS) was conducted on a Thermo Fisher Scientific K-Alpha spectrometer equipped with Al Kα (hv = 1486.6 eV) radiation. All peaks were corrected by setting the C1s peak of 284.8 eV as the reference.

In situ diffuse reflectance Fourier transform infrared spectroscopy (DRIFTs) of CO chemisorption experiments were performed on a ThermoFisher Scientific FTIR spectrometer (Nicolet iS50) equipped with a mercury cadmium telluride (MCT) detector. Before test, the aqueous solution containing the catalysts was vacuum dried to remove water, and then used as sample for the DRFTs measurement.

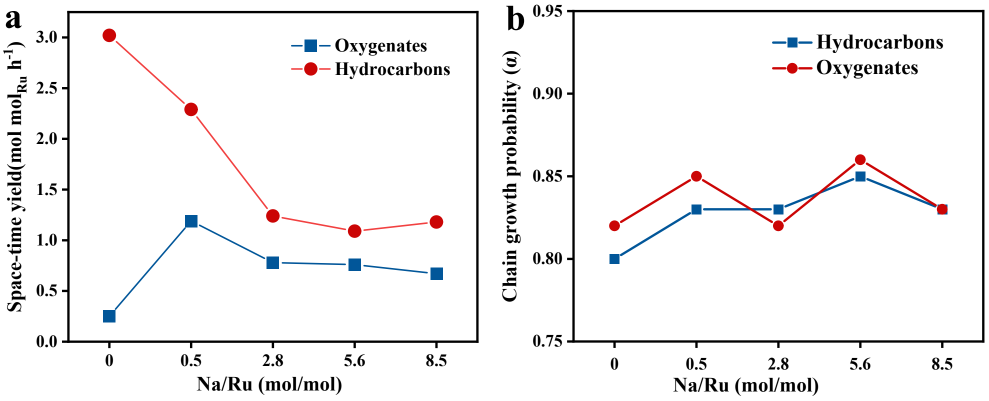

Fig. S1 Space-time yield (a) and chain growth probability (b) for hydrocarbons and oxygenates over samples with different Na/Ru molar ratio

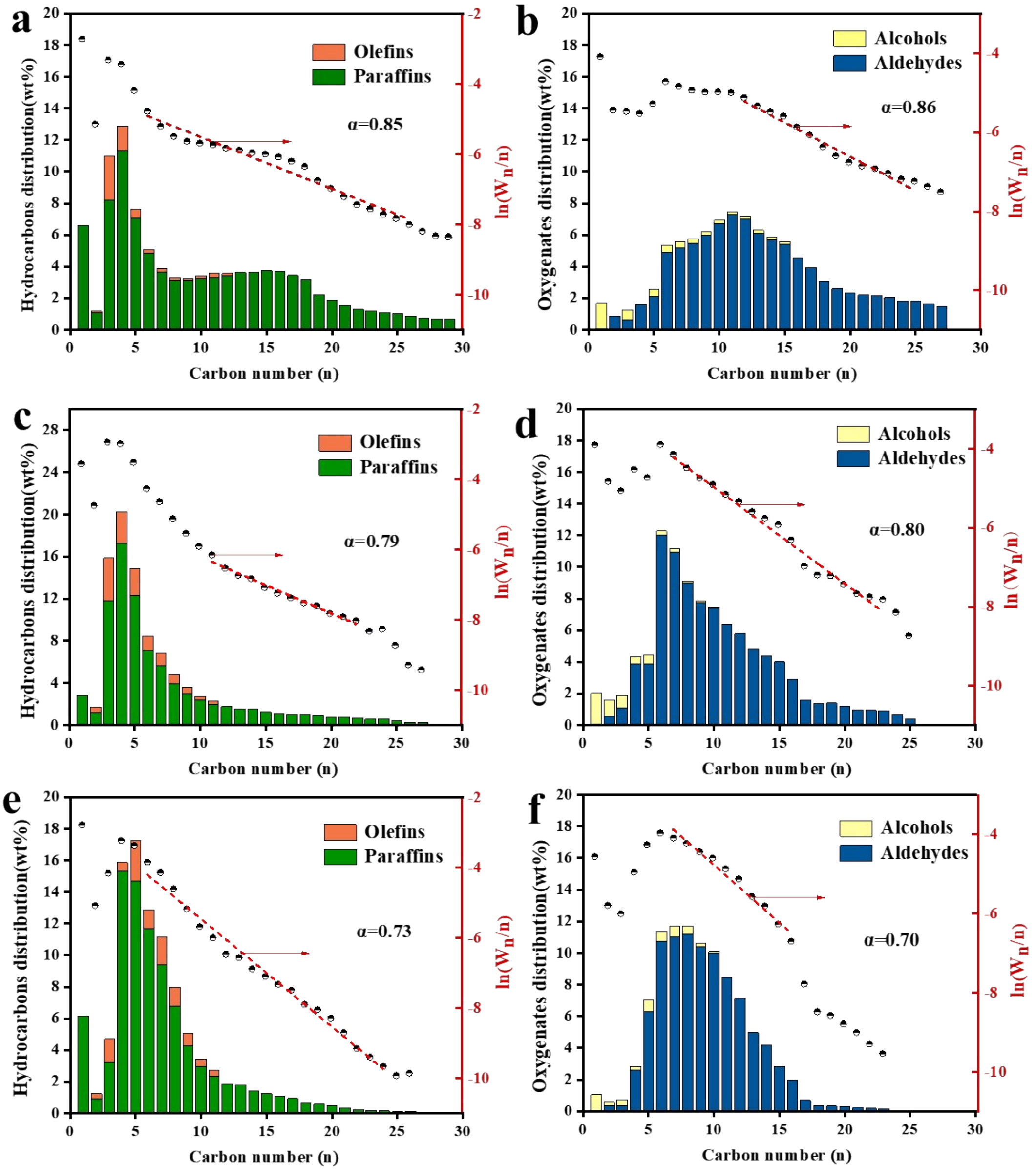

Fig. S2 Effect of anion of Na salts on ASF product distribution and chain growth probability (α). (a, b) Sample containing NaCl, (c, d) sample containing NaOH, (e, f) sample containing $NaNO_3$.

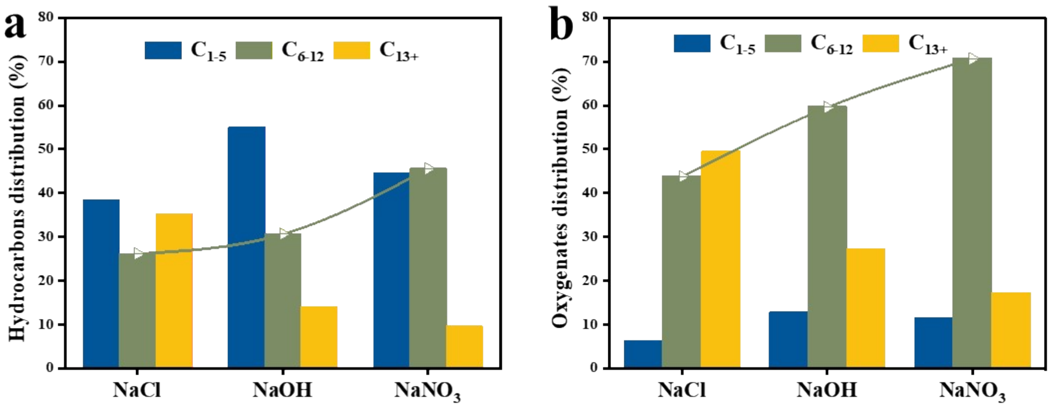

Fig. S3 Effect of anion of Na salts on distribution of hydrocarbons (a) and oxygenates (b).

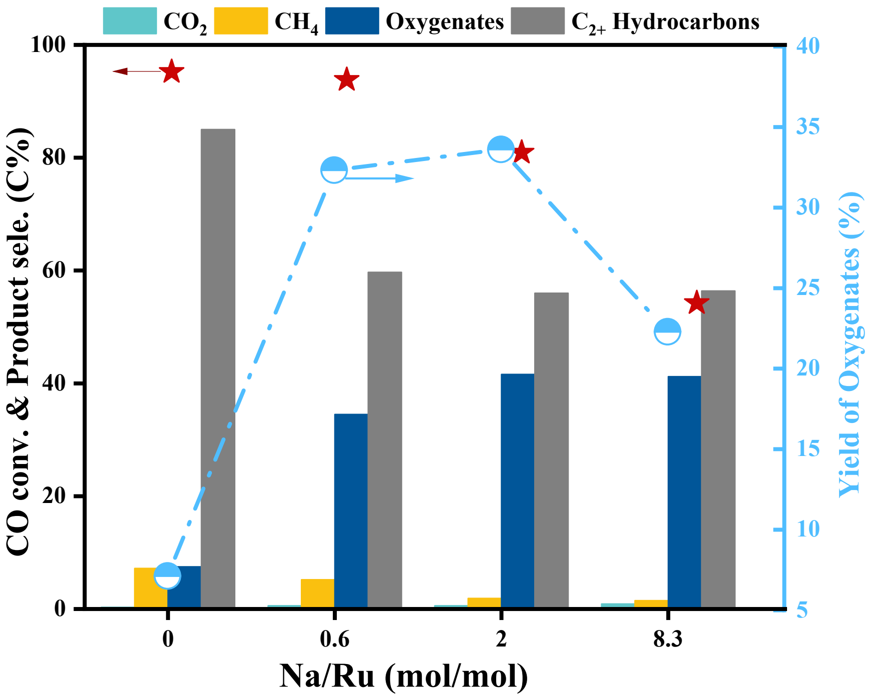

Fig. S4 Effect of concentration of NaOH on catalytic performance of Ru-PVP case.

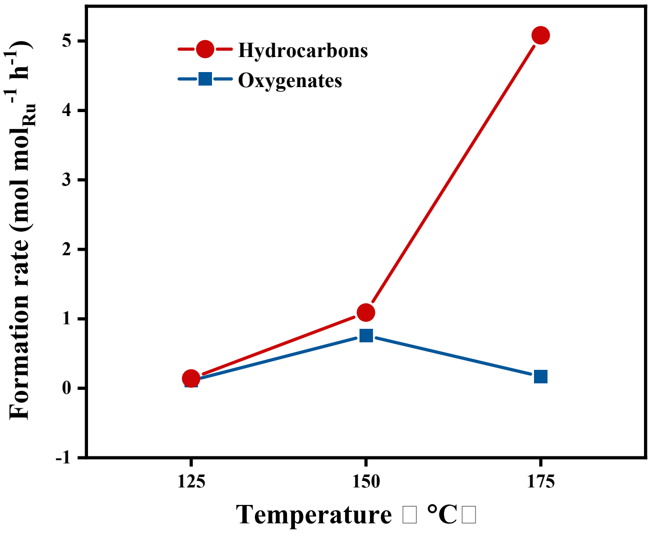

Fig. S5 Effect of reaction temperature on formation rate of products.

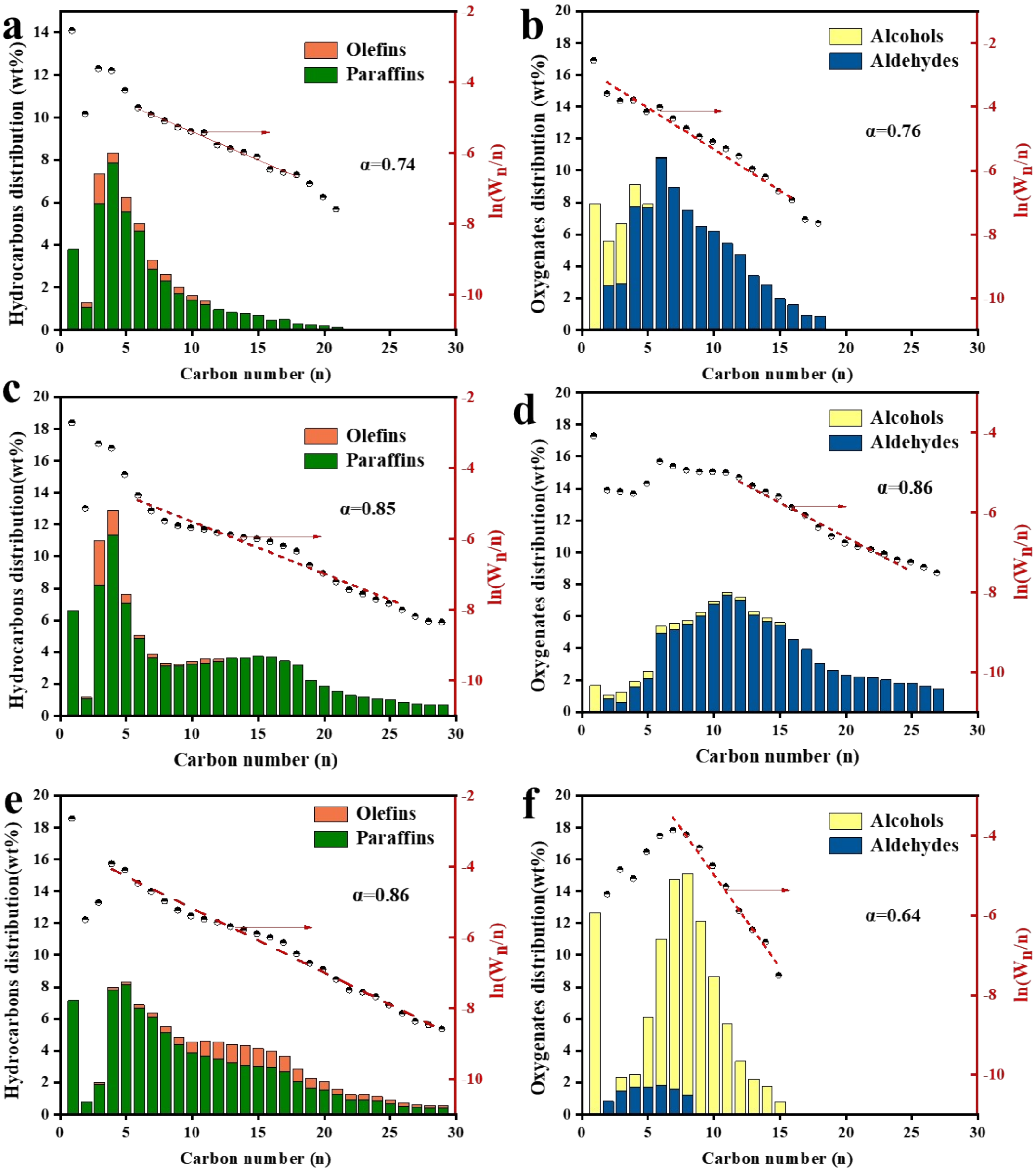

Fig.S6 Effect of reaction temperature on ASF plots and chain growth probability. (a) Hydrocarbons distribution at 125 °C, (b) Oxygenates distribution at 125 °C, (c) Hydrocarbons distribution at 150 °C, (d) Oxygenates distribution at 150 °C, (e) Hydrocarbons distribution at 175 °C, (f) Oxygenates distribution at 175 °C.

Table S1. Fitted XPS result for the spent Ru-PVP and Ru-Na-PVP.

Catalyst	Fitted peak area		Ratio
	Ru^0	$Ru^{\delta+}$	$Ru^0/ (Ru^0 + Ru^{\delta+})$
Ru-PVP	6064.7	1147.28	0.84
Ru-Na-PVP	16258.58	3413.53	0.83